Dimensional, Geometrical, and Physical Constraints in Skull Growth

Johannes Weickenmeier,[1] Cedric Fischer,[1,2] Dennis Carter,[1] Ellen Kuhl,[1] and Alain Goriely[3]

[1]*Department of Mechanical Engineering, Stanford University, Stanford, California 94305, USA*
[2]*Department of Mechanical and Process Engineering, ETH Zurich, 8092 Zurich, Switzerland*
[3]*Mathematical Institute, University of Oxford, Oxford OX2 6GG, United Kingdom*

After birth, the skull grows and remodels in close synchrony with the brain to allow for an increase in intracranial volume. Increase in skull area is provided primarily by bone accretion at the sutures. Additional remodeling, to allow for a change in curvatures, occurs by resorption on the inner surface of the bone plates and accretion on their outer surfaces. When a suture fuses too early, normal skull growth is disrupted, leading to a deformed final skull shape. The leading theory assumes that the main stimulus for skull growth is provided by mechanical stresses. Based on these ideas, we first discuss the dimensional, geometrical, and kinematic synchrony between brain, skull, and suture growth. Second, we present two mechanical models for skull growth that account for growth at the sutures and explain the various observed dysmorphologies. These models demonstrate the particular role of physical and geometrical constraints taking place in skull growth.

A fascinating observation in developmental morphogenesis is the highly interdependent growth of multiple tissues to create well-formed organs and organisms. A striking example of this synchronized growth process is found in the parallel development of the brain and skull [1–4]. Exactly 100 years ago, in the first edition of his essay "On Growth and Form", d'Arcy Thompson already marveled at the smoothness of this growth process of which he says: "It becomes at once manifest that the modifications of jaws, brain-case, and the regions between are all portions of one continuous and integral process" [[5], p. 771].

Here, following in the footsteps of d'Arcy Thompson, we are interested in the physical description of the cranial vault bones shown in Fig. 1. At birth, these different bones are joined by fibrous cartilaginous tissue to form the sutures [6]. Cranial vault expansion is primarily achieved by *suture growth*, a form of accretion similar to the processes found in crystal, coral, and seashell growth [7]. For the skull, rapid bone deposition occurs in ossification sites within sutures. Located at the edge of the individual bone plates, the growth sites move perpendicular to the orientation of sutures in order to accommodate the developing brain and to ensure that suture width remains nearly constant [6]. Complex signaling pathways regulate intramembranous ossification in these growth sites, which are made up of undifferentiated rapidly dividing mesenchymal cells that, if triggered, directly differentiate into osteoblasts, which lay down the extracellular collagenous matrix that mineralizes into new flat bones [8]. The main stimulus is believed to originate from mechanical loading: the growing brain induces stretching in the collagenous fibers within the sutures, which triggers the differentiation of mesenchymal cells into osteoblasts while inhibiting ossification within the suture itself [9–11].

The secondary growth mode, *surface growth*, takes place on both surfaces of the calvaria and results in remodeling of the bone shape and overall bone thickness increase [12]. It is believed that the mechanical loading of the dura mater by means of brain-growth-related intracranial pressure increase and line tension within the periosteum due to membrane stretch play a crucial role in triggering these highly localized growth mechanisms [13].

Here, we first use scaling relationships to understand the interdependence of the three basic growth modes: volumetric expansion of the brain, surface growth of the bones, and line growth along the suture. Second, we model regular and pathological growth by considering the evolution of these processes in three-dimensional geometries.

Dimensional constraints.—We consider a simple geometric model of a uniformly expanding skull such that it is a dilation of its initial shape [14]. The skull surface $\mathcal{S}$ with area A tightly encloses a brain of volume V, as shown in Fig. 2. Assuming that the intracranial volume only increases by edge growth, the problem is to understand the constraints between bone deposition at the edge, surface remodeling, and volumetric growth of the brain. Since the shape only changes by dilation, we can express the area A and volume V at any time t through a single characteristic cranial length $r = r(t)$ (e.g., the radius, head circumference, or width) so that

$$A(t) = C_a r^2(t), \qquad V(t) = C_v r^3(t), \qquad (1)$$

where C_a and C_v are constants that only depend on the shape. If the shape remains constant, then the ratio $A^3/V^2 = C_a^3/C_v^2$ is constant in time.

The sutures follow a set of curves on $\mathcal{S}$ with total arc length L, given by $L(t) = 2C_l r(t)$, where C_l only depends
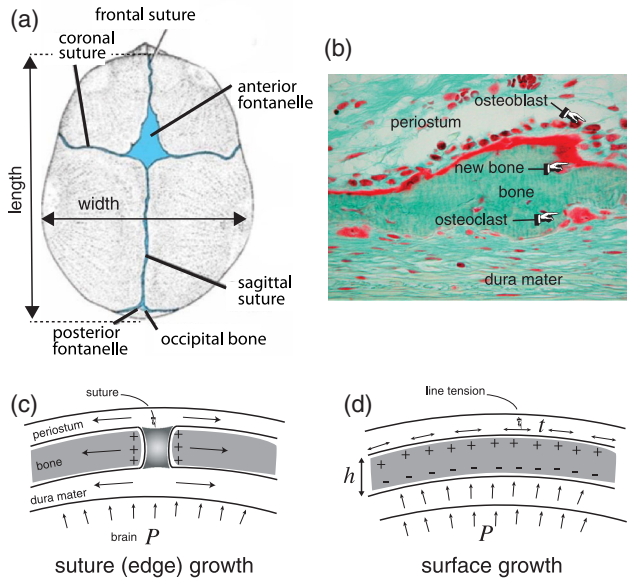
FIG. 1. Cranial skull in the newborn. (a) The calvaria is composed of the bones that can be seen from the top. (b) Bone histology: the inner layer (bottom) is composed of the dura mater and osteoclasts (large multinucleated cells), and the upper layer (top) is populated by osteoblasts (smaller cuboidal cells of typical size 20–30 μm), in which new bone deposition is observed (picture courtesy of the Maurice Mueller Institute, Bern). (c) Primary growth is achieved at the edge of the suture and is induced by the tension between calvarial bones. (d) Surface growth is induced by accretion on the outer surface (induced by tension) and by resorption on the inner surface (induced by pressure).

on the curves (the factor 2 reflects the fact that there are 2 sides to each suture). Let γ be the deposition rate at the edge with dimension length/time. Assuming that area increases only through edge deposition, we have $\dot{A} = \gamma L = 2\gamma C_l r$. From (1), we also have $\dot{A} = 2C_a r \dot{r}$; hence $\dot{r} = \gamma C_l / C_a$. Similarly, we can write the rate of volumetric growth expressed as newly grown volume per time as $\Gamma = \dot{V} = 3C_v r^2 \dot{r}$ so that

$$\gamma = \frac{C_a}{3C_l C_v^{1/3}} V^{-2/3}\Gamma. \tag{2}$$

This relationship imposes a very strict constraint between two completely different growth processes. Assuming that the shape of the skull does not change, the deposition rate γ must change in time and remain proportional to $V^{-2/3}\Gamma = \dot{V}V^{-2/3}$ at all times.

The increase in area by edge growth is not sufficient to obtain a dilation of the initial shape. To maintain the shape of a surface up to a dilation, the surface is remodeled through surface growth. To capture this effect, we endow the surface with a thickness h as shown in Fig. 2 so that at time t, $h_p = h_p(t)$, where $p \in \mathcal{S}$ is an arbitrary point on the midsurface $\mathcal{S}$. The resorption and accretion of the inner ($-$) and outer ($+$) surfaces happen at a rate $\delta_- > 0$ and $\delta_+ > 0$,
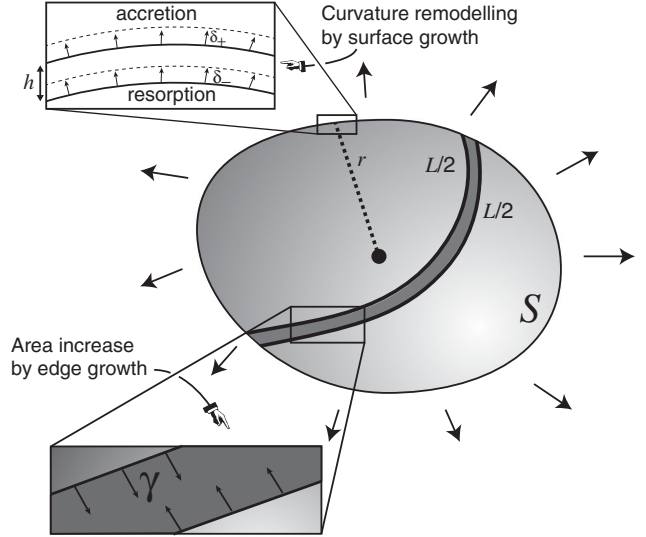

FIG. 2. Scaling of cranial growth. The surface $\mathcal{S}$ increases by edge growth at the suture. The curvature of the midsurface $\mathcal{S}$ changes through surface accretion and resorption.

both expressed as length/time, and possibly depending on the location. The rate of change of the thickness is $\dot{h}_p = \delta_+ - \delta_-$, and the thickness remains constant if $\delta_+ = \delta_-$. At a point p, in a direction $\mathbf{t}$ tangential to the surface, the radius of curvatures R can be expressed with respect to the characteristic length r as $R = C_c r$, where C_c is a constant independent of the size (but possibly depending on both p and $\mathbf{t}$). The rate of change of this curvature radius is $\dot{R} = C_c \dot{r} = C_c \gamma C_l / C_a$. It can also be expressed as a process of resorption and accretion so that $\dot{R} = \delta = (\delta_+ + \delta_-)/2$, where δ is a rate of remodeling (it changes the local curvature without necessarily increasing the mass). In order to maintain the shape during growth, we must have

$$\delta C_a = 2\gamma C_c C_l. \tag{3}$$

The shape parameters $\{C_a, C_v, C_l, C_c\}$ may change during development, as evident in mice and rats where the newborn skull elongates drastically after birth. In humans, however, the shape or the cranial vault remains mostly spherical. For instance, the *cephalic index*, defined as the percentage of the cranial vault's width w by its length l (see Fig. 1), does not vary much through growth: in healthy humans, it is typically between 76 and 81 [15,16]. Therefore, the constraints (2) and (3) imply that the three different growth processes, volumetric growth (Γ), edge growth (γ), and thickness remodeling (δ) must be tightly regulated in normal development.

Mechanical constraints.—It has been shown that bone growth and bone deposition rates in growth sites, such as sutures, strongly depend on the mechanical environment [14]. We consider skull growth between $t = 1$ to 24 months of age. At the kinematic level, the deposition rate γ follows an exponential decay [14] $\gamma \approx 3.5\exp(-0.1t)$ μm/month.

During the same period, a typical skull radius evolves linearly from $r(1) = 51$ mm to $r(24) = 76$ mm, and the thickness approximately triples from an initial $h(1) = 1.6$ mm within the first 4 years. At the mechanical level, we assume that the material is homogeneous and isotropic so that the tissue stress is also the stress at the cellular level. Assuming that the skull is a thin shell under internal pressure P acting on a spherical cap of radius r, the principal stress (the force per unit area acting across the skull thickness) is given by $\sigma = rP/(2h)$. Assuming further that the pressure exerted on the suture scales with the intracranial pressure in time, there is only a change of a factor of $3/2$ from 1 month to 4 years of age. Using the previous estimates, we conclude that the stress acting on the suture decreases by a factor of less than 2 during that period. Since there is little change in stress but dramatic change in the deposition rate, this estimate shows that stress-driven growth cannot be, by itself, the only driver of edge growth. Therefore, either biochemical production during that period is regulated (so that less new bone material is produced for the same stimulus), and/or growth is driven by another physical quantity. A possible candidate is strain. Bone production is a relaxation process that systematically removes stress during growth. Assuming an isotropic linear elastic response for the suture, the strain is $\epsilon = Pr(1 - \nu)/(2hE)$, where $\nu \approx 0.28$ is the Poisson's ratio that does not change significantly during growth. Henderson *et al.* [14] estimate that E increases by a factor of 50 from month 1 to 48. The strain decreases by the same amount in that time, and strain is therefore a better candidate for a growth law. At the cellular level, it would imply that it is the cell stretch that regulates osteoblast activity as observed in cellular assays [17].

Craniosynostosis.—Given the interdependent growth processes of the brain and skull, several skull growth pathologies appear when an individual or multiple cranial sutures fuse prematurely [18]. Such malformations, known as *craniosynostoses*, may lead to significant dysmorphologies and bear the risk of raised intracranial pressure, impaired cerebral blood flow, impaired vision and hearing, and cognitive impairment [8]. The etiology of this congenital disease is poorly understood since there are many unknown interactions between mechanical stimuli and molecular signaling pathways that regulate the ossification of sutures [19]. Little experimental data exist with regards to bone deposition rates of particular sutures, mechanical or genetic triggers that initiate bone deposition, mechanical properties of bone, and the actual signal for suture closure and ossification [13].

Here, we study the role of geometrical and mechanical constraints using two- and three-dimensional models to investigate suture growth patterns. In particular, we show that the geometry of premature suture ossification determines the clinically observed dysmorphologic skull shapes. We use the cephalic index as a quantitative measure for the
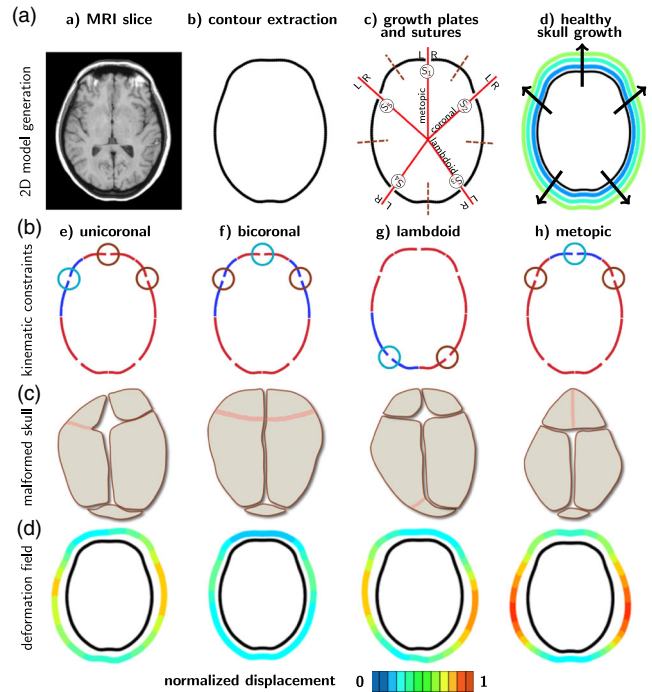

FIG. 3.   The two-dimensional skull growth model includes ten separate sections corresponding to the five major bone plates. (a) Synostosis occurs when sections are merged. (b) Depending on the type of synostosis, we restrict growth to selected sections. (c) Observed characteristic dysmorphological skull shapes. (d) Predicted skull contours and normalized skull displacements.

comparison of clinically observed and numerically predicted skull deformations. During healthy skull growth in infants, the cephalic index remains nearly constant [20].

Two-dimensional model.—We extract the skull contour of the largest transverse cross-sectional area from a newborn's magnetic resonance brain scan [Fig. 3(a)]. We scale the contour to a healthy cephalic index of 78 [12], divide it into ten individual sections, and discretize it by 194 growing beam elements (see Supplemental Material [21]). The healthy growing skull expands concentrically outwards, which we model through kinematic constraints on the sutures, shown by the red lines in Fig. 3(c). This configuration of suture lines ensures that the cranial index remains nearly constant when all bone sections grow under healthy conditions. We model growth through suture edge growth and remodeling by surface growth as a unidirectional homogeneous expansion along the principal axis of each beam element. Using child growth standards [22], we prescribe an increase of head circumference by 30% during the first 12 months of life. All bone sections marked red in Figs. 3(e)–3(h) grow by 30%, sections marked in blue do not grow at all, and all suture nodes move along the suture lines. We evaluate the growing skull shape on the basis of the normalized displacement field, which describes the distance between the deformed and undeformed contour, normalized by the maximum displacement observed in

TABLE I. Cephalic indices of two- and three-dimensional models for synostosis and the clinically observed average [20].

	Unicoronal	Bicoronal	Metopic	Lambdoid	Sagittal
2D	86.04	82.40	90.54	87.41	⋯
3D	87.83	93.49	78.18	84.97	68.13
clinical	84.44	94.16	81.49	88.09	69.98

the simulations. We observe that the kinematic constraint of respective sutures forces skull deformations in opposing regions of the skull and leads to malformations comparable with clinical observations, as shown in Fig. 3. Our simulations nicely predict the highly asymmetric deformation for the unicoronal [Fig. 3(e)] and lambdoid [Fig. 3(g)] cases. Fixation of the left lambdoid suture enhances the distortion of the contour [Fig. 3(c)]. The model also captures the often-observed pronounced widening but marginal lengthening of the skull, as well as the significant bulging of the frontal bone from fusion of the metopic suture [Fig. 3(h)]. The resulting cephalic indices for all four malformations, summarized in Table I, agree well with clinical data averaged over 104 synostoses [20].

Three-dimensional model.—As shown in Fig. 4, we approximate the skull as an ellipsoid with a cephalic index of 78 and 13 distinct regions representing the sutures and fontanelles (see Supplemental Material [21]). Suture edge growth is associated with the progressive formation of new bone material at the edge of the bone plates, and therefore moves in the direction normal to the edge. Based on this scheme, the metopic and sagittal sutures are primarily responsible for a widening of the skull (red patches), while coronal and lambdoid sutures lengthen the skull (yellow patches). The anterior and posterior fontanelles are at the intersection of multiple sutures and are considered to contribute to growth in both primary directions (purple patches). We model the growth of these patches as orthotropic in-plane growth [26,27] and simulate it using our custom-designed finite-element subroutine [28]. Lengthening and widening of the skull are governed by two growth rates, γ^l and γ^t. The only free parameter of the simulation, their ratio $\gamma^l/\gamma^t = 2.11$, is selected such that it preserves a cephalic index of 78 at a circumference growth of 30% within 12 months [22], see Fig. 4(a).

The three-dimensional skull growth model allows us to simulate all major synostoses, including scaphocephaly from premature sagittal suture fusion. The simulations are analyzed with respect to normalized displacements and the cephalic index. Maximum displacement in all six simulations is observed for fusion of the lambdoid suture [Fig. 4(d)] due to normal growth of the frontal part of the skull. The coronal and metopic sutures lead to a widening of the frontal bone, while the occipital bone remains rather rounded.

The individual malformation patterns of synostosis are captured by our model. The healthy skull shows largest
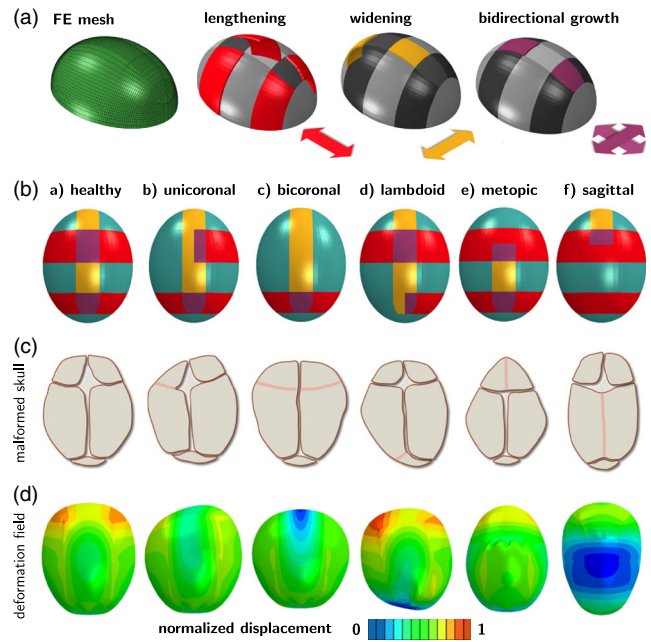

FIG. 4. The three-dimensional skull growth model includes 13 distinct regions corresponding to four sutures, two fontanelles, and five bones. (a) The model with the finite element mesh has three growth directions along the arrows: skull lengthening (red patches), skull widening (yellow patches), and area growth (purple patches). (b) Depending on the type of synostosis, we restrict suture and fontanelle growth to obtain the clinically observed malformations. (c) Observed characteristic dysmorphological skull shapes. (d) Predicted skull contours and normalized skull displacement field.

absolute area growth with all sutures growing and a concentration of bone formation in the frontal part of the skull. Length and width of the skull grow homogeneously, and therefore preserve the cephalic index. All other simulations experience lesser growth due to inactive suture regions but show an accentuation of deformation in synostosis-specific regions of the skull.

In unicoronal synostosis, the right frontal bone bulges outward, while the occipital bone maintains its rounded shape [Fig. 4(b)]. Bicoronal synostosis leads to the most severe inhibition of skull growth despite an excessive widening of the frontal skull [anterior brachycephaly, Fig. 4(c)]. One-sided lambdoid fusion leaves frontal bone growth nearly unaffected while leading to a significant asymmetric distortion of the skull and is associated with a noticeable flattening of the occipital bone [posterior plagiocephaly, Fig. 4(d)]. Growth of the metopic suture ensures sufficient frontal bone growth during the rapid growth period of the frontal brain in early life. Premature fusion leads to a keel-shaped deformity that the model clearly captures [trigonocephaly, Fig. 4(e)]. Finally, fusion of the sagittal suture, one of the most frequently diagnosed synostoses, leads to a severe skull malformation including significant lengthening and narrowing [scaphocephaly, Fig. 4(f)].

Table I summarizes the computationally predicted cephalic indices of our individual two- and three-dimensional simulations and shows remarkable agreement with the clinical data averaged over 104 cases of synostosis [20].

Discussion.—Skull growth and craniosynostosis are regulated at the biochemical level by extremely complex signaling pathways and genetic mutations. Yet, the coupling between growth processes of different dimensions—line, surface, and volume—implies that there must be a tight *global* regulation of the growth processes as to obtain a given final shape. Our physical analysis further supports the general understanding of skull growth and confirms that mechanics must be a key stimulus for this process and simple physical estimates further suggest that strain is a natural candidate to regulate this synchrony. The particular geometric role of the relative arrangement of the early cranial vault bones and the sutures appear clearly in our two- and three-dimensional growth models. Indeed, without a single fitting parameter, we show that idealized geometries give good agreement between numerically predicted and clinically observed cephalic indices as well as remarkable qualitative consistency in skull shape. Whereas our two-dimensional model is a simple model used to illustrate the interplay between growth, geometry, and mechanics, our three-dimensional ellipsoidal model can be coupled to biochemical processes in order to analyze several open questions in clinical practice, such as the impact of different bone growth rates, the relative magnitude of mechanical and biochemical stimuli during normal skull growth, and optimal dimensions of surgically reopened sutures. Our physics-based model is also a tool to study fundamental questions in developmental biology associated with the universality and optimality of cranial design in the evolution of mammalian skulls.

[1] D. R. Carter and G. S. Beaupre, *Skeletal Function and Form: Mechanobiology of Skeletal Development, Aging, and Regeneration* (Cambridge University Press, Cambridge, 2007).
[2] J. T. Richtsmeier and V. B. DeLeon, Orthod. Craniofac. Res. **12,** 149 (2009).
[3] J. T. Richtsmeier, K. Aldridge, V. B. DeLeon, J. Panchal, A. A. Kane, J. L. Marsh, P. Yan, and T. M. Cole, J. Exp. Zool. **306B,** 360 (2006).
[4] B. J. Nieman, M. C. Blank, B. B. Roman, R. Mark Henkelman, and K. J. Millen, Physiol. Genomics **44,** 992 (2012).
[5] D. W. Thompson, *On Growth and Form* (Cambridge University Press, Cambridge, 1917).
[6] L. A. Opperman, Dev. Dyn. **219,** 472 (2000).
[7] A. Goriely, *The Mathematics and Mechanics of Biological Growth* (Springer-Verlag, New York, 2017).
[8] A. Goriely, M. G. D. Geers, G. A. Holzapfel, J. Jayamohan, A. Jerusalem, S. Sivaloganathan, W. Squier, J. A. W. van Dommelen, S. Waters, and E. Kuhl, Biomech. Model. Mechanobiol. **14,** 931 (2015).
[9] M. L. Moss and R. W. Young, Am. J. Phys. Anthropol. **18,** 281 (1960).
[10] D. H. Enlow, *Facial Growth* (WB Saunders Company, publication city, 1990).
[11] L. A. Opperman, Dev. Dyn. **219,** 472 (2000).
[12] G. Morriss-Kay and A. O. M. Wilkie, J. Anat. **207,** 637 (2005).
[13] J. T. Richtsmeier and K. Flaherty, Acta Neuropathol. **125,** 469 (2013).
[14] J. H. Henderson, M. T. Longaker, and D. R. Carter, Bone (N.Y.) **34,** 271 (2004).
[15] N. Bayley, Hum. Biol. **8,** 1 (1936).
[16] A. S. Dekaban, Annals of Neurology **2,** 485 (1977).
[17] P. Müller, A. Langenbach, A. Kaminski, and J. Rychly, PLoS One **8,** e71283 (2013).
[18] D. Johnson and A. O. M. Wilkie, European Journal of human genetics : EJHG **19,** 369 (2011).
[19] V. Kimonis, J. A. Gold, T. L. Hoffman, J. Panchal, and S. A. Boyadjiev, Semin. Pediatr. Neurol. **14,** 150 (2007).
[20] J. F. Wilbrand, U. Bierther, T. Nord, M. Reinges, A. Hahn, P. Christophis, P. Streckbein, C. Kähling, and H. P. Howaldt, J. Craniomaxillofac. Surg. **42,** 634 (2014).
[21] See Supplemental Material at http://link.aps.org/supplemental/10.1103/PhysRevLett.118.248101, which includes Refs. [22–25], for details and different versions of the two- and three-dimensional models.
[22] WHO Multicentre Growth Reference Study Group, *WHO Child Growth Standards: Head Circumference-for-Age, Arm Circumference-for-Age, Triceps Skinfold-for-Age and Subscapular Skinfold-for-Age: Methods and Development* (World Health Organization, Geneva, 2007).
[23] E. K. Rodriguez, A. Hoger, and A. D. McCulloch, J. Biomech. **27,** 455 (1994).
[24] E. Kuhl, J. Mech. Behav. Biomed. Mater. **29,** 529 (2014).
[25] *Abaqus 6.16. Analysis User's Manual*, Dassault Systemes (2016).
[26] M. A. Holland, T. Kosmata, A. Goriely, and E. Kuhl, Math. Mechan. Solids **18,** 561 (2013).
[27] S. Göktepe, O. J. Abilez, and E. Kuhl, J. Mech. Phys. Solids **58,** 1661 (2010).
[28] A. M. Zöllner, M. A. Holland, K. S. Honda, A. K. Gosain, and E. Kuhl, J. Mech. Behav. Biomed. Mater. **28,** 495 (2013).